

Stochastic Models of Vesicular Sorting in Cellular Organelles

Quentin Vagne, Pierre Sens

April 15, 2022

Abstract

The proper sorting of membrane components by regulated exchange between cellular organelles is crucial to intra-cellular organization. This process relies on the budding and fusion of transport vesicles, and should be strongly influenced by stochastic fluctuations considering the relatively small size of many organelles. We identify the perfect sorting of two membrane components initially mixed in a single compartment as a first passage process, and we show that the mean sorting time exhibits two distinct regimes as a function of the ratio of vesicle fusion to budding rates. Low ratio values leads to fast sorting, but results in a broad size distribution of sorted compartments dominated by small entities. High ratio values result in two well defined sorted compartments but is exponentially slow. Our results suggests an optimal balance between vesicle budding and fusion for the rapid and efficient sorting of membrane components, and highlight the importance of stochastic effects for the steady-state organization of intra-cellular compartments.

Author Summary

An important function of the membrane-bound organelles along the endocytic and secretory transport pathways of eukaryotic cells is the sorting of proteins and lipids traveling across the cell. This sorting occurs predominantly through molecular recognition during individual transport steps, namely the packing of these molecules into protein-coated vesicles budding from a donor compartment, and the fusion of these vesicles with an acceptor compartment. We have developed a stochastic model for the sorting of membrane components based on selective vesicle budding and fusion, which identifies the occurrence of perfect and irreversible sorting as a first passage process controlled by stochastic fluctuations. We found two qualitatively distinct regimes of fast and slow sorting for high and low values of the ratio of vesicle budding to fusion rates. When analyzing the structure of the sorted compartments, we found again two distinct regimes with a dispersed (vesicular) phase and a condensed (compartmentalized) phase for high and low values of the ratio of budding to fusion rates. We conclude that the rapid sorting of membrane components into well-defined compartments requires a subtle balance between vesiculation and fusion rates, for which we provide a phase diagram.

Introduction

The hallmark of eukaryotic cells is their compartmentalization into specialized membrane-bound organelles. These organelles carry out specific functions and are characterized by specific physical

and biochemical properties, while constantly exchanging components with one another through the budding and fusion of small transport vesicles [1]. Exchange between organelles is tightly regulated, leading to directional intracellular transport along well-defined routes, the secretory and endocytic pathways [2]. One important function of the intracellular organelle network is the sorting of membrane components which are then dispatched to their proper location [3, 4, 5]. This process is regulated by molecular recognition during vesicle budding and fusion, and involves different kinds of membrane-associated proteins. The formation of the protein coats that control vesicle budding [6, 7] and the activity of tethers and SNAREs that mediate vesicle fusion [4, 8] are affected by membrane composition. This machinery is orchestrated by membrane components that define the identity of the organelles' membrane, such as members of the Rab GTPases family [9, 10]. In particular, Rabs control the homotypic fusion between membrane compartments with similar composition of Rabs, both in the endosomal network [11], and in the Golgi apparatus [12]. Although many of the molecular players contributing to the intracellular organization have been identified, we are still far from understanding how the complex and dynamical intra-cellular architecture emerges from the self-organization of individual molecules [1]. The interplay between vesicle budding and fusion poses a number of interesting questions regarding how organelles can robustly maintain distinct compositions while constantly exchanging material. Several theoretical studies have investigated such questions in recent years, mostly focusing on steady-state, time averaged properties of dynamical compartments exchanging material [13, 14, 15, 16, 17, 18]. It has been shown in particular that given sufficiently strong specificity of the budding and fusion transport mechanisms, one expects spontaneous symmetry breaking and the appearance of stable interacting compartments with distinct compositions [13, 15]. The inherently stochastic nature of intracellular transport however has been much less explored [19, 20]. The importance of fluctuations appears clearly when considering the typical organelle size along the transport pathways. An endosome or a Golgi cisterna has a membrane area of about $0.2 - 1 \mu\text{m}^2$, while the transport vesicles responsible for exchange within and between compartments are typically of diameter about $50 - 100 \text{ nm}$. The budding/fusion of a few tens of vesicles is thus enough to completely renew the membrane composition of a compartment. Indeed, the size and composition of early endosomes show strong fluctuations, which are correlated with budding and fusion events [11]. Such system must thus be described as a stochastic process undergoing strong fluctuations around an average state. In this study, we develop a fully stochastic description of the sorting of membrane components by mean of the emission and fusion of vesicles targeting specific membrane components, a process of direct relevance to intra-cellular organization. We show that both the average sorting time of two membrane species initially mixed into a single compartment, and the size distribution of the sorted compartments depend critically on the ratio of vesicle fusion to budding rates. We conclude that the efficiency of a sorting mechanism designed to sort an initially mixed compartment into a few well defined pure compartments requires an optimization of the relative rates at which these two transport processes occur.

Results

General features of the model

In this paper we use the term organelle in a very general sense, referring to any membrane-bound compartment capable of vesicular exchange. Transport vesicles are assumed to have a fixed area s , taken as the unit size of the system. We consider that the organelle size, defined by its area S ,

can vary only through the budding and fusion of vesicles or other organelles. It is thus defined as an integer number of vesicles $N = S/s$, which decreases by steps of unit size one for each vesicle budding, and increases by an integer number of unit one steps during fusion.

- Identity: The membrane of different organelles contain different types of lipids and proteins that can coexist in a given membrane and whose exchange between organelles is regulated [21]. Some proteins are permanently embedded within the lipid bilayer and are transported with the lipids, while others (such as Rab GTPases [22]) undergo energy consuming cycles between active (membrane-bound) and inactive (cytosolic) states. All these molecules define the global chemical identity of membranes. We account for membrane variability in a coarse-grained and simplified way by defining two generic types of membrane (A, B), and we allow a particular membrane compartment to contain a mixture of type A and B membranes. For simplicity, we coarse-grain the membrane composition at the size of a transport vesicle. A compartment's membrane thus consists of N sites that can be either of type A or B , and its composition is completely defined by the number of sites N_A and N_B of type A and B , respectively.

- vesicle emission and organelle fusion: Both vesicle emission from a donor compartment and vesicle fusion with an acceptor compartment are highly specific for lipids and proteins. In vivo, vesicular emission is controlled by coat complexes that assemble at the membrane in composition-specific fashion and bend it into the shape of a vesicle [23]. The fusion mechanisms are specifically influenced by interactions with membrane components including matching pairs of SNAREs [4]. This is implemented here in the following way. In the analytic part of the work, we consider that vesicle emission only affects the type B (mature) membrane component, and is characterized by a rate (per site)

$$K_{\text{site}} = Kf(\phi) \quad f(\phi) \equiv \frac{\epsilon\phi}{1 - \phi + \epsilon\phi} \quad (1)$$

where the parameter K controls the vesicular emission rate, ϵ represents the selectivity of vesicle emission for the B component, and $\phi \equiv N_B/N$ is the fraction of B component in the membrane. We extend this model to allow the vesicular export of both membrane components in the numerical simulation. As explained in the *Methods* section (Selectivity of vesicle emission), Eq.(1) amounts to considering that coat formation occurs at a rate K , that a coat selectively bud-off from the compartment if it interacts with a membrane of type B , and that the affinity of the coat to type B component is characterized by a Boltzmann factor ϵ (≥ 1). The average flux of vesicle leaving an organelle of size N and composition ϕ per unit time is thus $NKf(\phi)$. Regarding vesicle fusion, we implement a general homotypic fusion mechanism based on the idea that fusion is possible only between membrane sites of the same type. We assume that any two compartments 1 and 2 of mixed compositions ϕ_1 and ϕ_2 in the system meet at a rate k_f (independent of their size), and fuse with a probability given by the probability that two random sites of their membranes are identical, leading to the average fusion rate between two compartment:

$$k_{\text{fusion}} = k_f g(\phi_1, \phi_2) \quad g(\phi_1, \phi_2) \equiv \phi_1\phi_2 + (1 - \phi_1)(1 - \phi_2) \quad (2)$$

We consider an isolated system initially made of a single organelle containing a mixture of A and B membrane types, and we study the dynamics of the stochastic process by which selective vesicle budding and homotypic fusion lead to pure A and B compartments. The main control parameters are the ratio of fusion to budding rates k_f/K , the initial size N of the mother compartment, and its initial composition ϕ_0 . We study the process sketched in Fig.1, seeking to answer two questions: (1) What is the mean first passage time to irreversible separation of A and B components, and (2) what is the size distribution of the pure A and B compartments resulting from the sorting process.

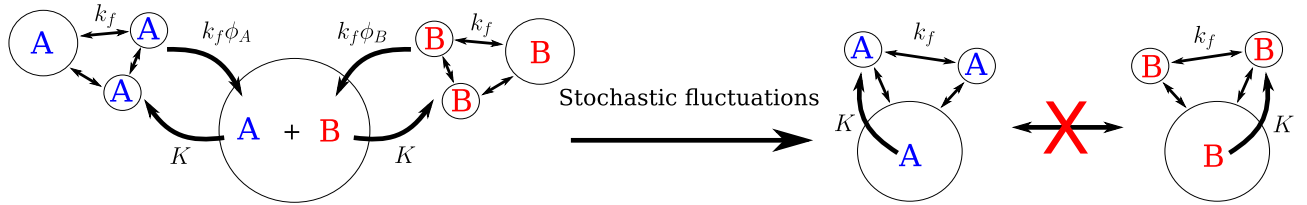


Figure 1: **Sketch of the sorting mechanism.** A “mother” compartment contains both A and B membrane components, which are individually exported by vesicle budding. Secreted vesicles with the same identity fuse with one another to create pure A and B compartments, and may fuse back with the mother compartment with a composition-dependent rate. Pure A and B compartments do not fuse together. Stochastic fluctuations lead to the permanent separation of A and B components into two independent distributions of pure compartments.

Mean Sorting Time

We consider an isolated system with a fixed number N_A and N_{B0} of membrane sites of type A and B , which are initially mixed into a single compartment, and study the sorting of A and B component by selectively extracting B from the mixed compartment through vesicle budding. The sorting process is slowed down by the fact that newly-formed B compartments can fuse back with the mixed compartment, but within the homotypic fusion scheme (Eq.(2)), pure A and B compartments (*i.e.* $\phi_1 = 1$ and $\phi_2 = 0$) cannot fuse together, so that perfect and permanent sorting will necessarily be achieved at some point, when stochastic fluctuations completely remove all B components from the mother compartment. In this section, we first derive the mean sorting time analytically by making the simplifying assumptions that all B components removed from the mother compartment aggregate into a single, pure B compartment. This is done both in the continuous (infinite size) approximation and in the case where finite-size effects are relevant. We identify two distinct regimes, fast and slow sorting, as a function of the ratio k_f/K of fusion to budding rates and of the fraction $\phi_0 = N_{B0}/(N_A + N_{B0})$ of B sites in the system.

The assumptions that there are only two compartments in the system is justified by the fact that the average fusion flux toward the mother compartment from a size distribution N_n of pure B compartment of size n is only sensitive to the total size $\sum_n nN_n$ of the distribution. However, the size of the concentration jump following each fusion event is influenced by the actual size distribution, so the assumption should only be qualitatively valid if the size distribution is broad. Comparison of our analytical results with stochastic numerical simulations show that this subtlety can to some extent be accounted for by including the probability that a budded vesicle directly fuses back with the mother compartment. The full steady-state size distribution of the pure B compartments, in which budding and fusion also occurs, is discussed in the next section.

Continuous approximation

If the system size is large: $N_{B0} \gg 1$, the number of B sites $N_B(t)$, or equivalently the fraction of B site in the mother compartment, $\phi(t) = N_B(t)/(N_A + N_B(t))$ may be treated as a deterministic continuous variable between fusion events. Using Eq.(1), the temporal evolution of the $\phi(t)$, and the time t_0 for complete sorting of B components (when the mother compartment reaches $\phi(t_0) = 0$) satisfy:

$$\frac{d\phi}{dt} = -K(1 - \phi)f(\phi) \quad t_0 = \frac{1}{K} \int_0^{\phi_0} \frac{d\phi}{(1 - \phi)f(\phi)} \quad (3)$$

Note that depending on the actual expression of $f(\phi)$, the value of t_0 might not be finite. For instance, if $f(\phi \ll 1) \propto \phi$, as in Eq.1, this leads to $t_0 = \infty$. This is an artifact of the continuous model, and we will see in the next section that t_0 is always finite as long as $f(\phi) > 0 \forall \phi > 0$ in more realistic discrete models.

In addition to the continuous decrease of ϕ through vesicle emission, the compartment containing all the emitted vesicles may fuse back with the mother compartment at any instant with a probability density $k_f \phi(t)$. This defines a stochastic process where $\phi(t)$ continuously decreases towards zero, but is submitted to stochastic jumps that reset the system to its initial configuration ϕ_0 . Since the total number of jumps is independent of the waiting time between each jump, the average time (mean first passage time - MFPT) to complete separation may be written

$$\tau = t_0 + \langle n_{jump} \rangle \langle t_{jump} \rangle \quad (4)$$

where $\langle n_{jump} \rangle$ is the mean number of jump and $\langle t_{jump} \rangle$ is the mean waiting time between two jumps.

As shown in the *Methods* section (*Mean sorting time in the continuous limit*), the mean first passage time to full separation can be expressed as:

$$\tau = t_0 + \frac{1}{K} \int_0^{\phi_0} \frac{d\phi}{(1-\phi)f(\phi)} \left(\exp \left[\frac{k_f}{K} \int_0^{\phi} d\phi' \frac{\phi'}{(1-\phi')f(\phi')} \right] - 1 \right) \quad (5)$$

Asymptotic behaviors can be extracted from this expression. When $k_f \ll K$, fusion is very unlikely, the integral in the RHS of Eq.(5) vanishes, and the isolation time is deterministic: $\tau \simeq t_0$ given by Eq.3. In the other limit where fusion is frequent: $k_f \gg K$, the value of τ is dominated by the short-time fusion events. Performing a Taylor expansion of the integrand for $\phi \simeq \phi_0$ yields the approximate expression:

$$\lim_{k_f \gg K} \tau = \frac{1}{k_f \phi_0} \exp \left[\frac{k_f}{K} \int_0^{\phi_0} d\phi \frac{\phi}{(1-\phi)f(\phi)} \right] \quad (6)$$

One thus expects the sorting time to cross over from being insensitive to the fusion rate k_f when $k_f \ll K$, to increasing exponentially with the fusion rate when $k_f \gg K$.

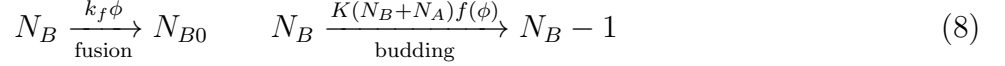
The asymptotic result given Eq.(6) must be refined in order to properly reproduce the simulation results presented below. The previous derivation was done assuming that there are only two compartments in the system, the mixed ‘‘mother’’ compartment, containing a fraction $\phi(t)$ of B components, and the pure B compartment containing all the emitted vesicles. However, there are temporarily three compartments in the system just after a vesicle budding event, and the emitted vesicle has a probability $\phi(t)/(1+\phi(t))$ to fuse back with the mother compartment rather than with the B compartment. Consequently, the effective budding rate is reduced compared to Eq.(1), which can be accounted for by replacing $f(\phi)$ by $f(\phi)/(1+\phi)$ in the previous derivation. The numerical simulations discussed below were performed in the limit of strong coat selectivity: $\epsilon \gg 1$ to reduce the number of parameters. In this case, $f(\phi) = 1$ and the sorting time takes the asymptotic expressions:

$$\begin{aligned} \lim_{k_f \ll K} \tau &= t_0 = \frac{1}{K} \ln \frac{1}{1-\phi_0} \\ \lim_{k_f \gg K} \tau &= t_0 + \frac{1}{k_f \phi_0} \exp \left(2 \frac{k_f}{K} \left[\ln \frac{1}{1-\phi_0} - \phi_0 \left(1 + \frac{\phi_0}{4} \right) \right] \right) \end{aligned} \quad (7)$$

These asymptotic expressions are expected to be valid for sufficiently large systems only, since they rely on the hypothesis that $N_B(t)$ can be treated as a continuous variable.

Discrete case

It is possible to compute the MFPT τ exactly for the discrete system and for any size $N_0 = N_A + N_{B0}$, within the hypothesis that there are only two compartments in the system. In this case the stochastic evolution of $N_B(t)$ is driven by the transitions:



Following a computation scheme explained in the *Methods* section (*Mean sorting time in the discrete limit*), we can obtain an equation for the mean sorting time $\tau(n)$ for reaching $n = 0$ if $n \in [0, N_{B0}]$ is the starting value of N_B at time $t = 0$:

$$\begin{aligned} \text{For } n < N_{B0}, \quad -1 &= K(n + N_A)f(\phi(n))(\tau(n-1) - \tau(n)) + k_f \phi(n)(\tau(N_{B0}) - \tau(n)) \\ -1 &= K(N_{B0} + N_A)f(\phi(N_{B0}))(\tau(N_{B0}-1) - \tau(N_{B0})) \end{aligned} \quad (9)$$

Using the knowledge that $\tau(0) = 0$ and the recursive treatment explained in the *Methods* section, we obtain a final expression for the mean sorting time:

$$\tau = \tau(N_{B0}) = \frac{1}{K} \sum_{i=1}^{N_{B0}} \frac{1}{(i + N_A)f(\phi(i))} \prod_{j=1}^{i-1} \left(1 + \frac{k_f}{K} \frac{\phi(j)}{(j + N_A)f(\phi(j))} \right) \quad (10)$$

where $\phi(j) = j/(N_a + j)$. This expression gives access to the variation of the sorting time τ with the system size. It is useful to consider its behavior for small and large values of k_f/K , to leading order:

$$\begin{aligned} \text{For } k_f/K \ll g_m(N, \phi_0), \quad K\tau &\approx \sum_{i=1}^{N_{B0}} \frac{1}{(i + N_A)f(\phi(i))} \\ \text{For } k_f/K \gg g_M(N, \phi_0), \quad K\tau &\approx \left(\frac{k_f}{K} \right)^{N_{B0}-1} \frac{1}{\phi_0} \prod_{i=1}^{N_{B0}} \frac{\phi(i)}{(i + N_A)f(\phi(i))} \end{aligned} \quad (11)$$

A power-law dependence $K\tau \sim (k_f/K)^{\phi_0 N}$ of the mean sorting time with the fusion rate is predicted in the high fusion regime. The ranges of validity for the asymptotic regimes are given by the functions $g_m(N, \phi_0)$ and $g_M(N, \phi_0)$, derived in the Appendix (*Mean sorting time in the discrete limit*). We find $g_m(\phi_0, N) = \tilde{g}_m(\phi_0)$, independent of N , and $g_M(N, \phi_0) \simeq N^2 \tilde{g}_M(\phi_0)$. There is thus a cross-over region $\tilde{g}_m(\phi_0) \ll k_f/K \ll N^2 \tilde{g}_M(\phi_0)$, which is very broad for large systems, between the constant and power-law regimes of sorting time. This region corresponds to the exponential dependency $K\tau \sim e^{k_f/K}$ obtained for large systems ($N \rightarrow \infty$, Eq.(7)).

Detailed study for $f = 1$

Again we consider the case of perfect sorting ($f = 1$). The asymptotic behavior for $k_f \ll K$ is given simply in this case by:

$$\tau \approx \frac{1}{K} \sum_{i=1}^{N_{B0}} \frac{1}{i + N_A} = \frac{1}{K} \left(\sum_{n=1}^{N_A + N_{B0}} \frac{1}{n} - \sum_{n=1}^{N_A} \frac{1}{n} \right) \quad (12)$$

We recognize harmonic series showing that the discrete solution converges towards the corresponding limit in Eq.(7) for large values of N_A and N_{B0} . To treat the case $k_f \gg K$, we must consider

the fate of an emitted vesicle as in the continuous case. This time, due to the discreteness the case $N_B = N_{B0}$ is special because the vesicle cannot fuse with another compartment. Instead of using $f = 1$ we use:

$$\begin{aligned} f(\phi) &= \frac{1}{1 + \phi} \text{ when } N_B < N_{B0} \\ f(\phi) &= 1 \text{ when } N_B = N_{B0} \end{aligned} \quad (13)$$

Then we can compute τ numerically using Eq.10.

Simulation results

The simulation procedure is described in the *Methods* section (*Simulation scheme*). Fig.2 shows the values of the dimensionless mean sorting time $K\tau$ obtained from simulations with $f = 1$ and compared with the discrete and continuous analytical models. The dimensionless sorting time depends only on the ratio k_f/K and on the initial composition N_A and N_{B0} . The fast

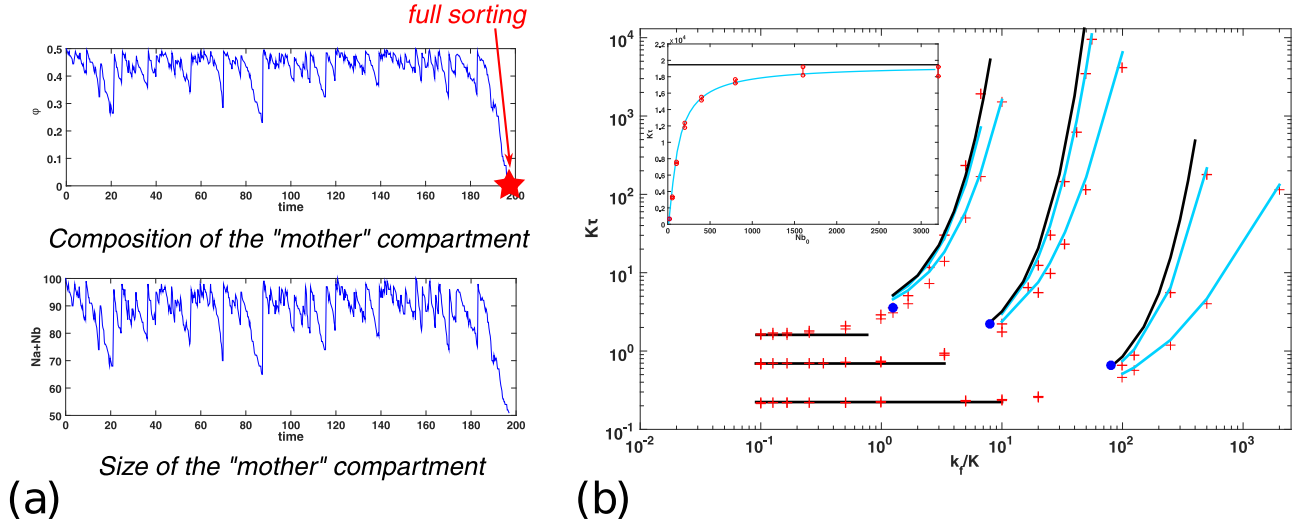


Figure 2: Sorting time. (a) Typical time trace for the mother compartment composition (fraction of B component ϕ - top) and size (bottom). Full sorting occurs when $\phi = 0$ (red star). (b) Dimensionless mean first passage time $K\tau$ as a function of the ratio of fusion to budding rate k_f/K for different initial compositions and sizes. Three groups of curves are visible and correspond to different initial compositions (from left to right: $\phi_0 = 0.8, 0.5$ and 0.2). The simulation results (red crosses) are shown for two different initial compartment sizes in each case (lower data: $N_0 = 20$, upper data: $N_0 = 100$). The black curves show the asymptotic behavior for $N_0 \rightarrow \infty$ as obtained using the continuous approximation for $K \gg k_f$ and $K \ll k_f$ (Eq.(7)). The light blue curves show the results of the discrete model using Eq.(10) adapted to the situation $k_f \gg K$ using Eq.(13), and the transition from fast to slow sorting (Eq.(15)) are shown as blue dots. The inset shows the evolution of the mean first passage time $K\tau$ as a function of N_{B0} for $\phi_0 = 0.5$ and $k_f/K = 50$. The color code is the same than the one of the main graph. Each simulation result is an average over many independent simulations. The error bars represent the standard deviation of this average.

and slow sorting regimes predicted analytically, namely $K\tau$ independent of k_f and exponential or power-law in k_f/K , depending on the system's size, are indeed observed. The transition between

them occurs for a value of k_f/K that depends on the surface fraction ϕ_0 . Such behavior has been observed in computer simulations before [19], but without further study of its origin. Our analytical treatment fully explains this transition, which can be understood without the need of a stochastic model by considering that both vesicle budding and compartment fusion are continuous processes. Sorting is a slow process if the system reaches a long-lived state where the fusion of the sorted compartments with the mother compartment balances vesicle budding. In the mean-field description, this corresponds to a steady-state. Let us write an equation for the time evolution of the average value of N_B in the mother compartment. This quantity decreases because of vesicle budding at a rate $K(N_A + n)$, and increases because any of the $N_{B0} - N_B$ components that have been emitted fuses back with the mother compartment at a rate $k_f\phi$, regardless of whether the emitted component are gathered in a single compartment or in many. The average temporal evolution of $N_B(t)$ is thus given by:

$$\dot{N}_B = -K(N_A + N_B) + k_f \frac{N_B}{N_A + N_B} (N_{B0} - N_B) \quad (14)$$

This equation admits a steady-state with $N_B \neq 0$ only under the following condition:

$$\frac{k_f}{K} \geq \frac{4(1 - \phi_0)}{\phi_0^2} \quad (15)$$

One can see in Fig.2 (blue dots) that this condition quantitatively predicts the cross-over between fast and slow sorting. This result can be extended to the case where both A and B components can bud from the compartment. The evolution of the average value of A and B components (with initial values N_{A0} and N_{B0}) then reads:

$$\begin{aligned} \dot{N}_A &= -K(N_A + N_B) + k_f \frac{N_A}{N_A + N_B} (N_{A0} - N_A) \\ \dot{N}_B &= -K(N_A + N_B) + k_f \frac{N_B}{N_A + N_B} (N_{B0} - N_B) \end{aligned} \quad (16)$$

Obtaining the condition for the existence of a steady-state analytically with Eq.(16) is cumbersome, so we only show numerical results in Fig.4. Of particular interest is the case where the mother compartment is initially symmetrical: $N_{A0} = N_{B0}$. Its average evolution given by Eq.(16) is also symmetrical, and the transition from fast to slow sorting can be predicted analytically to be when $k_f/K \geq 1/4$.

Size distribution of the sorted compartments

The assumption that all emitted vesicles of B component gather into a single compartment is clearly an oversimplification and one expects a distribution of size for the sorted compartments. Solving the full sorting problem while accounting for this size distribution, which varies dynamically together with the composition of the mother compartment, is very challenging. One can however understand the role of the budding and fusion rates on the distribution of compartment size by looking at the steady state that is reached after full sorting of the B components. If both A and B components undergo budding and fusion, the size distributions of the compartments they form are described by the same equations.

At the mean-field level, the size distribution N_n (the number of compartments of size n) of pure B compartment evolving via vesicle budding and compartment fusion satisfies the Master

equations [24, 16]:

$$\frac{dN_n}{dt} = \frac{k_f}{2} \sum_{m=1}^{n-1} N_m N_{n-m} - k_f N_n \sum_{m=1}^{\infty} N_m + K(n+1)N_{n+1} - KnN_n + \delta_{n,1}K \sum_{m=1}^{\infty} N_m m \quad (17)$$

with the constraint that the total amount of B components $N_B \equiv \sum_{n=1}^{\infty} nN_n$ is fixed. It is shown in the *Methods* section (*Steady-state cluster size distribution*) that in the mean-field limit ($N_B \rightarrow \infty$), the dynamics described by Eq.(17) leads to a steady-state with a broad size distribution. The computer simulations presented in Fig.3 show that for finite-size systems, a single macro-compartment containing most of the components dominates the size distribution if $k_f/K > 1$. This can be understood qualitatively by comparing the typical growth and evaporation rates of a compartment of size n . The evaporation rate is given by Kn and, provided that $n \ll N_B$, the average growth rate by fusion is $k_f \sum_n nN_n = N_B k_f$. At steady-state, the two rates should balance, leading to a typical size $n = N_B k_f / K$, consistent with the exact solution of Eq.(17) (see *Methods*). This solution is clearly inconsistent if $k_f/K \geq 1$, since it predicts a compartment size larger than the total system's mass, indicating the appearance of a macro-compartment. If one

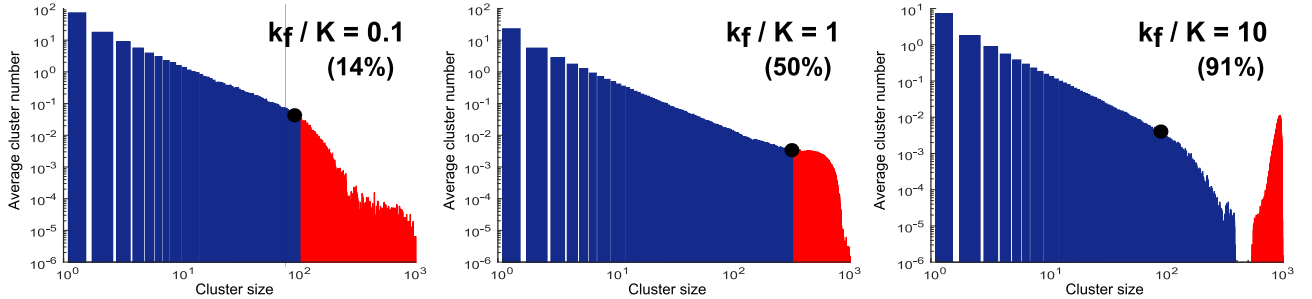


Figure 3: **Size distributions.** Steady-state size distribution of one-component compartments undergoing fusion at a rate k_f and shedding vesicles at a rate K , for different values of the fusion to budding rate ratio k_f/K . The total membrane area is $N = 10^3$. The red part of the distribution represents the single, largest compartment. The fraction of the total area it contains (given in parenthesis) is consistent with the theoretical estimate of Eq.(18). The typical size of the small compartments, estimated using Eq.(20), is also displayed on each graph (black dots).

assumes that such a compartment exists and contains a fraction ρ of the total mass N_B , this compartment grows due to the fusion of the smaller compartments, with a flux $k_f(1 - \rho)N_B$, and shrinks due to budding with a flux $K\rho N_B$. Balancing these two fluxes leads to the steady-state fraction

$$\rho = \frac{k_f}{k_f + K} \quad (18)$$

of the total mass N_B . The typical size of the distribution of small compartments can be obtained with the same reasoning. The size $n(t)$ of a compartment created by vesicle budding at $t = 0$ satisfies:

$$\dot{n} = k_f(1 - \rho)N_B - Kn \quad n(0) = 1. \quad (19)$$

Small compartments grow until they fuse with the macro-compartment, which occurs in a typical time $1/k_f$. Therefore the typical small compartment size can be estimated by $n(t = 1/k_f)$:

$$n(t = 1/k_f) = \rho N_B \left(1 - e^{-\frac{1-\rho}{\rho}}\right) + e^{-\frac{1-\rho}{\rho}} \quad (20)$$

Eqs.(18,20) are good quantitative estimate of the full size distribution computed numerically, and shown on Fig.3.

Discussion

The highly dynamical nature of intracellular organization requires the exchanges processes between organelles to be tightly regulated in order to yield robust directed flows of material across the cell. The precise sorting of lipids and proteins is crucial to this organization, and occurs by molecular recognition at the different steps of transport, mostly during the budding and fusion of transport vesicles. While much effort has been devoted to unraveling this process at the molecular level, much remains to be understood to bridge the gap between molecular interactions and self-organization at the scale of the entire cell. This requires the use of statistical models where molecular interactions are treated in a coarse-grained fashion and self-organization results from a statistical average over many molecular events. Stochasticity has an important impact on the dynamics of membrane-bound organelles, as many organelles along the cellular transport pathways are not much larger than the transport vesicles themselves.

In this work, we have focused on one crucial function of cellular organelles, which is to sort components via selective (composition-dependent) budding and fusion events. Specifically, we compute the time needed to fully separate two components initially mixed into a mother compartment by vesicle budding and fusion. If the component B can be removed by vesicle budding, and in the absence of fusion, the composition in B of the mother compartment decreases exponentially with a time scale equal to the inverse budding rate. The sorting of component B is thus very fast, but component B is then dispersed in a large number of small vesicles that are unable to fuse with one another. If fusion is allowed between compartments sharing the same identity, the budded vesicles are able to fuse with one another and form large compartments made solely of B components. On the other hand, the B vesicles and compartments may also fuse with the mother compartment, which slows down the sorting process dramatically. The resulting sorting time then strongly depends of the ratio of fusion to budding rate. The dependency is exponential for large compartments, and is a power law for small compartment (Eqs.(7,11)). There is thus a clear optimization problem to solve in order to obtain two (or a few) well sorted compartments containing only A or B components in a relatively short time. This is illustrated in Fig.4, where the boundaries between fast and slow sorting regimes are shown, together with the fraction of the sorted components that are contained into a single, large compartment. As an example, fast sorting of a binary mixture of membrane components of arbitrary composition is consistent with having up to 80% of the sorted components into single macro-compartments.

While the cell may to some extent be viewed as the steady-state of a complex, dynamical system, specific budding and fusion events, which are at the heart of its organization, are inherently stochastic processes. In the present study, the slow sorting regime corresponds to the existence of a steady-state in the mean-field formalism for which the mother compartment always remains mixed. A pure mean-field treatment of the sorting problem is thus unable to predict the sorting time in the full range of values of the ratio of budding to fusion rates. The strong fluctuations of the size and composition of early endosomes, before stochastic fluctuations lead to their full maturation into late endosomes [11] is a clear illustration of the need for a stochastic treatment of intra-cellular transport such as the one presented here for physiologically relevant values of the exchange rates controlling intra-cellular organization.

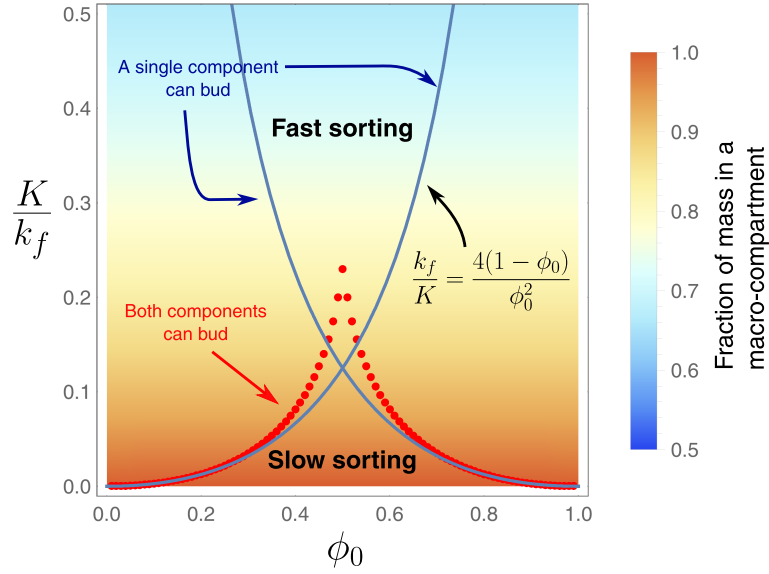


Figure 4: **Phase diagram.** Sorting phase diagram showing how the interplay between vesicular export and fusion influences the sorting time and the organization of the sorted components. The color background represents the fraction of the total area contained in a single, macro-compartment (Eq.(18)). The boundary between fast and slow sorting is indicated by the solid blue lines when only one component can be exported in budding vesicles (Eq.(15)), and by the red dotted line when both components can be exported. The rapid sorting of mixed components into well-defined sorted compartments can be obtained through the tuning of the ratio of K/k_f .

Methods

Selectivity of vesicle emission

The selective recruitment of membrane components into transport vesicles is permitted by their interaction with components of the protein coat complexes that shape the vesicles [6, 7]. One may attempt to model this phenomenon by considering that this selectivity is purely driven by equilibrium energetic interactions. We assume that such coat complex can form on any of the N sites on one compartment, and that there is an energy gain $-E < 0$ if a coat forms on any of the N_B sites occupied by type B membrane components. The Boltzmann factor $\epsilon = e^{E/k_b T} > 1$ associated to this gain is a tuning parameter for the selectivity of vesicles to type B components. At equilibrium, the probability for a given coat complex to be on a type B site is given by:

$$p_B = \frac{\epsilon N_B}{N - N_B + \epsilon N_B} \quad (21)$$

If the overall rate of coat formation and departure is proportional to the total membrane area and is a linear function of p_B (meaning that the actual vesicle emission requires the presence of type B membrane) we obtain this expression for the total number of vesicles emitted per unit time from an organelle :

$$KNp_B = \frac{K\epsilon NN_B}{N - N_B + \epsilon N_B} = \frac{K\epsilon N\phi}{1 + (\epsilon - 1)\phi} \quad (22)$$

Where the parameter K controls the vesicular emission rate. This corresponds to Eq.(1) for the net budding rate.

Mean sorting time in the continuous limit

We define the survival probability $p_S(t)$ which is the probability to reach the time t without having jumped, having started at ϕ_0 at time $t = 0$. The jumping rate being $k_f\phi(t)$, the equation satisfied by $p_S(t)$, and its solution, are:

$$\frac{dp_S}{dt} = -k_f\phi(t)p_S(t) \quad p_S(t) = e^{-\int_0^t k_f\phi(t')dt'} = e^{-\frac{k_f}{K} \int_{\phi_0}^{\phi(t)} \frac{\phi}{(1-\phi)f(\phi)} d\phi} \quad (23)$$

The probability of reaching $\phi = 0$ without experiencing a fusion event (a jump) is $p_0 \equiv p_S(t_0)$, hence the probability of experiencing exactly n jumps before complete separation is $p_n = p_0(1 - p_0)^n$. Consequently, the mean number of jumps is

$$\langle n_{jump} \rangle = \sum_{n=1}^{\infty} np_n = \frac{1 - p_0}{p_0} \quad (24)$$

For one jump, the probability density of the jumping time is $-\frac{dp_S}{dt}$ so the average jumping time is given by:

$$\langle t_{jump} \rangle = \frac{\int_0^{t_0} t \frac{dp_S}{dt}(t) dt}{\int_0^{t_0} \frac{dp_S}{dt}(t) dt} = \frac{-t_0 p_0 + \int_0^{t_0} p_S(t) dt}{1 - p_0} \quad (25)$$

Introducing Eqs.(24,25) in Eq.(4), we get the expression of the separation time:

$$\tau = \frac{1}{p_S(t_0)} \int_0^{t_0} p_S(t) dt \quad (26)$$

which is the one used in the text (Eq.(5)), after a change of integration variable from t to ϕ .

Mean sorting time in the discrete limit

Recursion relation

In this appendix we show how to obtain the classical equation on mean first passage times for a discrete one dimensional system submitted to a stochastic dynamics governed by transition rates. We consider a system described by a discrete variable $n \in \mathbb{N}$. The dynamics of n is stochastic and the transition rate from the configuration n to the configuration m is written $R_{n \rightarrow m}$. We are interested in the quantity τ_n which is the average time needed to reach the configuration 0 starting from configuration n . We call $p(n, t)dt$ the probability to reach 0 between t and $t + dt$ starting from n at $t = 0$. One can write an equation on the functions $p(n, t)$ by computing the probability to reach 0 at time $t + dt$ starting from n . In order to do this, during a time dt the system will either jump towards another configuration m or stay in n and then use a time t to reach the configuration 0. Mathematically written, it reads:

$$p(n, t + dt) = \sum_{m \neq n} R_{n \rightarrow m} dt p(m, t) + \left(1 - \sum_m R_{n \rightarrow m} dt\right) p(n, t) \quad (27)$$

This leads to a differential equation on $p(n, t)$:

$$\frac{\partial p(n)}{\partial t} = \sum_{m \neq n} R_{n \rightarrow m} (p(m, t) - p(n, t)) \quad (28)$$

Multiplying by t and integrating on the time leads to an equation for the mean first passage time τ_n to reach $n = 0$ starting at n , which is a classical result obtained in [25] p298-303 in the restricted case of one-step processes:

$$\forall n \in \mathbb{N} \quad -1 = \sum_{m \neq n} R_{n \rightarrow m} (\tau_m - \tau_n) \quad (29)$$

From the knowledge of a particular value of τ_n , usually $\tau_0 = 0$, one can use Eq (29) to obtain recursively the expression of τ_n , see below.

Mean first passage time

We want to compute $\tau(N_{B0})$ for a system characterized by the stochastic evolution Eq.(8). Rewriting Eq.(9) as:

$$\begin{aligned} \text{For } n < N_{B0}, \tau(n-1) &= -u_n - v_n \tau(N_{B0}) + \tau(n)(1 + v_n) \\ \tau(N_{B0}-1) &= -u_{N_{B0}} + \tau(N_{B0}) \end{aligned} \quad (30)$$

where u_n and v_n are defined by as:

$$u_n = \frac{1}{K(n + N_A) f(\phi(n))} \text{ and } v_n = \frac{k_f \phi(n)}{K(n + N_A) f(\phi(n))} \quad (31)$$

We use Eq.30 in a recursive manner starting from $\tau(0) = 0$:

$$\begin{aligned} \tau(0) = 0 &= -u_1 - v_1 \tau(N_{B0}) + (1 + v_1)(-u_2 - v_2 \tau(N_{B0}) + (1 + v_2)(\dots \\ &\dots - u_{N_{B0}-1} - v_{N_{B0}-1} \tau(N_{B0}) + (1 + v_{N_{B0}-1})(-u_{N_{B0}} + \tau(N_{B0}))) \dots \end{aligned} \quad (32)$$

In this way we can expand and obtain the following equality:

$$0 = - \sum_{i=1}^{N_{B0}} u_i \prod_{j=1}^{i-1} (1 + v_j) + \tau(N_{B0}) \left(\prod_{i=1}^{N_{B0}-1} (1 + v_i) - \sum_{i=1}^{N_{B0}-1} v_i \prod_{j=1}^{i-1} (1 + v_j) \right) \quad (33)$$

It can be shown by developing the products that:

$$\prod_{i=1}^{N_{B0}-1} (1 + v_i) = 1 + \sum_{i=1}^{N_{B0}-1} v_i \prod_{j=0}^{i-1} (1 + v_j). \quad (34)$$

This simplifies Eq (33) greatly, and the isolation time then reads:

$$\tau(N_{B0}) = \sum_{i=1}^{N_{B0}} u_i \prod_{j=0}^{i-1} (1 + v_j) \quad (35)$$

which leads to the final analytic expression used in the text (Eq.(10)).

Range of validity of the low fusion and high fusion regimes

Eq.(11) gives asymptotic expressions for the mean sorting time in the low fusion ($k_f/K \ll g_m(N, \phi_0)$) and high fusion ($k_f/K \gg g_m(N, \phi_0)$) regimes. The function g_m may be obtained by developing the product in Eq.(10) to first order in k_f/K , to obtain:

$$\prod_{j=1}^{i-1} \left(1 + \frac{k_f}{K} \frac{\phi(j)}{(j + N_A)f(\phi(j))} \right) \approx 1 + \frac{k_f}{K} \sum_{j=1}^{i-1} \frac{j}{(j + N_A)^2 f(\phi(j))} \quad (36)$$

The value of $g_m(N, \phi_0)$ is therefore given by:

$$g_m(N, \phi_0) = \frac{1}{\text{Max}_i \sum_{j=1}^{i-1} \frac{j}{(j + N_A)^2 f(\phi(j))}} = \frac{1}{\sum_{j=1}^{N_{B0}-1} \frac{j}{(j + N_A)^2 f(\phi(j))}} \quad (37)$$

For N large the sum can be estimated by an integral:

$$\sum_{j=1}^{N_{B0}-1} \frac{j}{(j + N_A)^2 f(\phi(j))} = \int_1^{N_{B0}} \frac{x dx}{(x + N_A)^2 f(x/(x + a))} = \int_{1/(N_A+1)}^{\phi_0} \frac{\phi d\phi}{(1 - \phi)f(\phi)} \quad (38)$$

The influence of the system's size is negligible provided $N_A \gg 1$, yielding the following expression:

$$g_m(N, \phi_0) = \tilde{g}_m(\phi_0) \quad \text{with} \quad \tilde{g}_m(\phi_0) = \frac{1}{\log\left(\frac{1}{1-\phi_0}\right) - \phi_0} \quad \text{when } f = 1 \quad (39)$$

We use the same kind of approximate reasoning in the case $k_f/K \gg 1$ large and we obtain:

$$g_M(N, \phi_0) = \text{Max}_i \sum_{j=1}^{i-1} \frac{(j + N_A)^2 f(\phi(j))}{j} \approx N^2 (1 - \phi_0)^2 \int_{1/(N_A+1)}^{\phi_0} \frac{d\phi}{\phi(1 - \phi)^3 f(\phi)} \quad (40)$$

This time g_M is expected to scale roughly with N^2 :

$$g_M(N, \phi_0) \simeq N^2 \tilde{g}_M(\phi_0) \quad (41)$$

with

$$g_M(N, \phi_0) \simeq N^2 \left(\phi_0 \left(4 - \frac{3}{2} \phi_0 \right) + (1 - \phi_0)^2 \log(N \phi_0) \right) \quad (42)$$

when $f(\phi) = 1$.

Steady-state cluster size distribution.

Starting with the mean-field equation Eq.(17), we define $t' = Kt$ and $c_n = N_n k_f / K$ which leads to purely numerical equations:

$$\frac{dc_n}{dt'} = \frac{1}{2} \sum_{m=1}^{n-1} c_m c_{n-m} - c_n \sum_{m=1}^{\infty} c_m + (n+1)c_{n+1} - nc_n + \delta_{n,1} \sum_{m=1}^{\infty} c_m m \quad (43)$$

This kind of Master equation, broadly referred to as variant of the Smoluchowski coagulation [26], have been studied extensively in the past [27]. A similar problem is studied in [28], but with a fission rate independent of the cluster size. In this case and in the mean-field regime ($N_B \rightarrow \infty$), a steady-state cluster distribution is observed only for $N_B < K/k_f$ while the distribution is dominated by a single large cluster that grows indefinitely if $N_B > K/k_f$. A stochastic version of this model has been developed in [29], in which compartment diffusion in space is explicitly modeled, that shows the same transition independently of the dimension. In order to compute a typical compartment size in our case, where the budding rate depends on the cluster size, we investigate the moments of the size distribution $m_n = \sum_k k^n c_k$. Mass conservation imposes $m_1 = \frac{k_f}{K} N_B = \text{constant}$. The moments can be obtained from derivatives of the generating function $g(z, t') = \sum_{n=1}^{\infty} z^n c_n(t')$. Using the equations on c_n we obtain the following equation for g :

$$\frac{\partial g}{\partial t'} = \frac{g^2}{2} - gm_0 + \frac{\partial g}{\partial z}(1-z) + zm_1 - c_1 \quad (44)$$

We can remove the dependency on c_1 using the function $h(z, t) = g(z, t) - g(1, t)$. the equation for h is:

$$\frac{\partial h}{\partial t'} = \frac{h^2}{2} + \frac{\partial h}{\partial z}(1-z) - m_1(1-z). \quad (45)$$

The steady-state solution that is monotonically increasing for $z \in [0, 1]$ and satisfies $h(1) = 0$ is

$$h(z) = -\sqrt{2m_1(1-z)} \frac{I_1\left(\sqrt{2m_1(1-z)}\right)}{I_0\left(\sqrt{2m_1(1-z)}\right)} \quad (46)$$

where I_0 and I_1 are Bessel functions [30]. This solution is defined for all values of m_1 , so there is no evidence of non equilibrium phase separation at the mean-field level. From this function $h(z)$ we can extract the first moments of the steady-state size distribution:

$$\begin{aligned} m_0 &= \sqrt{2m_1} \frac{I_1(\sqrt{2m_1})}{I_0(\sqrt{2m_1})} \approx \sqrt{2m_1} \text{ for } m_1 \rightarrow \infty \\ m_2 &= m_1 + \frac{m_1^2}{2} \\ m_3 &= \frac{m_1^3}{2} + \frac{3m_1^2}{2} + m_1 \end{aligned} \quad (47)$$

Consequently, in the limit $M \gg K/k_f$, the moments of the compartment size distribution, defined as $M_n = \sum_k k^n N_k$, satisfy: $M/M_0 \sim \sqrt{Mk_f/K}$ and $M_i/M_{i-1} \sim Mk_f/K$ for $i > 1$. This is consistent with a size distribution presenting a power law for small compartment size, and an exponential decay at a size $\sim Mk_f/K$ [31], which we take as the characteristic size of the distribution.

Simulation scheme

We make use of the Gillespie algorithm [32] to perform exact stochastic simulations of our system. The Gillespie algorithm is a general method that allows to compute statistically correct trajectories for a stochastic system. The system must be described by a discrete set S of states. Being in a given state $i \in S$ at time t , the system must have a probability $R_{i \rightarrow j} dt$ to jump from i to another

state j between t and $t + dt$. This definition is rather general, which allows the Gillespie algorithm to be applied in a variety of Physical contexts. Here the state space S is composed of all the possible distributions of compartments. A given state is defined as:

$$\{(N_A^1, N_B^1), (N_A^2, N_B^2), \dots, (N_A^N, N_B^N)\} \in S \quad (48)$$

In which N_A^i and N_B^i are the numbers of A sites and B sites in the compartment number i . The total number of compartment N is a dynamic quantity that varies because of fusion and fission events. Below is the list of all the allowed transitions between states together with their transition rates:

$$\begin{aligned} \text{Fusion of compartment } i \text{ with compartment } j &: k_f g(\phi_i, \phi_j) \\ \text{Fission from compartment } i &: K(N_A^i + N_B^i) f(\phi_i) \end{aligned} \quad (49)$$

After defining the system and its dynamics, the Gillespie algorithm can be employed to generate statistically exact trajectories using the following scheme:

1. Initialize a random number generator.
2. Initialize the system at $t = 0$ in a state Ω . Here we choose the state $\Omega = \{(N_A, N_{B0})\}$, meaning that we start with all the mass in one compartment.
3. Compute the sum Σ of all the transition rates out of the state $\Omega(t)$, and use it to generate the waiting time Δt before the next event using the distribution $\Sigma e^{-\Delta t \Sigma}$.
4. Choose randomly the nature of the event $\Omega(t) \rightarrow \Omega' \in S$ that happens, knowing that the probability of having $\Omega(t) \rightarrow \Omega'$ is given by $R_{\Omega(t) \rightarrow \Omega'} / \Sigma$.
5. Update the time to $t + \Delta t$ and the state Ω to the selected Ω' .
6. Loop back to state 3.

This scheme has been proved to generate trajectories that are exact in the sense that the probability for the program to generate a given trajectory is equal to the probability of observing this trajectory in the real system. In this paper we implemented this algorithm in the C language using the Mersenne Twister pseudo random number generator.

The first result obtained is the mean sorting time starting from a single compartment containing N_A and N_{B0} sites. In order to compute this quantity we performed a large number of simulations all identical apart from the initial state of the random number generator. We initialize the system at $t = 0$ with only one compartment and let the simulation run. After each time step we check for a complete sorting of the components, which is defined as having for all compartments i either $N_A^i = 0$ or $N_B^i = 0$. Once complete sorting happens the simulation is stopped and the time is registered. We perform a sufficiently large number of simulations to ensure that we obtain a satisfying estimate of this mean sorting time.

The next part consists in obtaining the steady-state compartment size distribution of a one-component system. This time we can perform only one simulation. We initialize the system at $t = 0$ with one compartment purely made of B components and of size N_B . We let the simulation run and we record snapshots of the size distribution at different (regularly spaced) time steps. By size distribution we mean the numbers n_i^k of compartments of size i in the snapshots number $k \leq N_{snap}$. We then compute the average number of compartments of size i which is

$\langle n_i \rangle = \sum_k n_i^k / N_{snap}$. Provided that N_{snap} is large enough we eliminate any dependency of the average on the initial distribution. The results obtained with this simulation scheme can be precisely compared with the results of the discrete model (Eq.(10)), as shown in Fig.2. Of particular interest is the dependency of the mean sorting time with the system's size, a property not accessible with the continuous approximation. This is also illustrated on Fig.2, where the simulation results for the average sorting time show excellent agreement with the stochastic model for all system's sizes.

References

- [1] Misteli T. The concept of self-organization in cellular architecture. *J Cell Biol.* 2001;155:181–185.
- [2] Kelly RB. Pathways of protein secretion in eukaryotes. *Science.* 1985;230(4721):25.
- [3] Mellman I. Endocytosis And Molecular Sorting. *Annu Rev Cell Dev Biol.* 1996;12:575–625.
- [4] Cai H, Reinisch K, Ferro-Novick S. Coats, Tethers, Rabs, and SNAREs Work Together to Mediate the Intracellular Destination of a Transport Vesicle. *Dev Cell.* 2007;12:671–682.
- [5] Jovic M, Sharma M, Rahajeng J, Caplan S. The early endosome: a busy sorting station for proteins at the crossroads. *Histol Histopathol.* 2010;25:99–112.
- [6] Mancias J, Goldberg J. Structural basis of cargo membrane protein discrimination by the human COPII coat machinery. *EMBO J.* 2008;27:2918.
- [7] Traub L. Tickets to ride: selecting cargo for clathrin-regulated internalization. *Nat Rev Mol Cell Biol.* 2009;10:583–596.
- [8] Chen YA, Scheller RH. SNARE-mediated membrane fusion. *Nature Reviews Molecular Cell Biology.* 2001;2(2):98–106.
- [9] F Schimmöller IS, Pfeffer S. Rab GTPases, Directors of Vesicle Docking. *J Cell Biol.* 1998;273:22161–22164.
- [10] Zerial M, McBride H. Rab Proteins as Membrane Organizers. *Nat Rev Mol Cell Biol.* 2001;2:107–117.
- [11] Rink J, Ghigo E, Kalaidzidis Y, Zerial M. Rab Conversion as a Mechanism of Progression from Early to Late Endosomes. *Cell.* 2005;122:735–749.
- [12] Pfeffer SR. How the Golgi works: A cisternal progenitor model. *P Natl Acad Sci Usa.* 2010;107:19614–19618.
- [13] Heinrich R, Rapoport TA. Generation of nonidentical compartments in vesicular transport systems. *J Cell Biol.* 2005;168:271–280.
- [14] Binder B, Goede A, Berndt N, Holzhutter H. A conceptual mathematical model of the dynamic self-organisation of distinct cellular organelles. *PloS one.* 2009;4(12):e8295.
- [15] Dmitrieff S, Sens P. Cooperative protein transport in cellular organelles. *Phys Rev E.* 2011;83:041923.

- [16] Foret L, Dawson J, Villaseñor R, Collinet C, Deutsch A, Bruschi L, et al. A General Theoretical Framework to Infer Endosomal Network Dynamics from Quantitative Image Analysis. *Curr Biol.* 2012;22:1381–1390.
- [17] Bressloff P. Two-pool model of cooperative vesicular transport. *Phys Rev E.* 2012;86:031911 1–10.
- [18] Ispolatov I, Müsch A. A Model for the Self-Organization of Vesicular Flux and Protein Distributions in the Golgi Apparatus. *PLoS Computational Biology.* 2013;9:e1003125.
- [19] Guo HGY, Linstedt A, Schwartz R. Discrete, continuous, and stochastic models of protein sorting in the Golgi apparatus. *Phys Rev E.* 2010;81:011914.
- [20] Bressloff P, Newby J. Stochastic models of intracellular transport. *Rev Mod Phys.* 2013;85:135–196.
- [21] Melser S, Molino D, Batailler B, Peypelut M, Laloi M, Wattelet-Boyer V, et al. Links between lipid homeostasis, organelle morphodynamics and protein trafficking in eukaryotic and plant secretory pathways. *Plant Cell Reports.* 2011;30(2):177–193. doi:10.1007/s00299-010-0954-1.
- [22] Stenmark H. Rab GTPases as coordinators of vesicle traffic. *Nature Reviews Molecular Cell Biology.* 2009;10(8):513–525. doi:10.1038/nrm2728.
- [23] Mahon HM, Mills I. COP and clathrin-coated vesicle budding: Different pathways, common approaches. *Curr Opin Cell Biol.* 2004;16:379–391.
- [24] Turner MS, Sens P, Succi ND. Nonequilibrium Raftlike Membrane Domains under Continuous Recycling. *Phys Rev Lett.* 2005;95:168301.
- [25] Kampen NGV. *Stochastic Processes in Physics and Chemistry.* Elsevier; 1992.
- [26] von Smoluchowski M. Drei Vorträge über Diffusion, Brownsche Molekular Bewegung und Koagulation von Kolloidteilchen. *Physik Z.* 1916;17:557–585.
- [27] Davies SC, King J, Wattis J. Self-similar behaviour in the coagulation equations. *J Eng Math.* 1999;36:57–88.
- [28] Krapivsky L, Redner S. Transitional aggregation kinetics in dry and damp environments. *Phys Rev E.* 1996;54:3553–3561.
- [29] Rajesh R, Majumdar SN. Exact phase diagram of a model with aggregation and chipping. *Physical Review E.* 2001;63(3):036114. doi:10.1103/PhysRevE.63.036114.
- [30] Abramowitz M, Stegun IA. *Handbook of Mathematical Functions.* Dover; 1964.
- [31] Vagne Q, Turner M, Sens P. Sensing Size through Clustering in Non- Equilibrium Membranes and the Control of Membrane-Bound Enzymatic Reactions. *PLoS ONE.* 2015;10:e0143470.
- [32] Gillespie DT. Exact stochastic simulation of coupled chemical reactions. *J Chem Phys.* 1977;81(25):2340–2361.